

# Surface Tension and Parachor Measurement of Low-Global Warming Potential Working Fluid cis-1-chloro-2,3,3,3-tetrafluoropropene (R1224yd(Z))

*Chieko Kondou, † Yukihiro Higashi, ‡ Shun Iwasaki, †*

†School of Engineering, Nagasaki University, 1-14 Bunkyo-machi, Nagasaki 852-8521, Japan

‡NEXT-RP in WPI-I2CNER, Kyushu University, 744 Motoooka, Nishi-ku, Fukuoka 819-0395, Japan

KEYWORDS: Surface tension, Parachor method, Refrigerant, R1224yd(Z)

## ■ ABSTRACT

This manuscript presents the accurate surface tension measurement of cis-1-chloro-2,3,3,3-tetrafluoropropene (R1224yd(Z), (Z)-CF<sub>3</sub>CF=CHCl) over the temperature range 266–340 K. The measurement was performed using the differential capillary rise. The expanded uncertainty at 95% confidence was estimated to be within 0.19 mN·m<sup>-1</sup>. Based on the measured data, the van der Waals-type correlation expressing the temperature dependence was obtained as  $\sigma = 57.02 (1 - T/428.69)^{1.265}$  [mN·m<sup>-1</sup>]. In addition, the parachor [ $P_{R1224yd(Z)}$ ] was determined as 207. The surface

tension values predicted by Miller and Thodos (Ind. Eng. Chem. Fund., 1963, 2.1, 78), Miqueu et al. (Fluid Ph. Equilibria, 2000, 172, 169), and Di Nicola et al. (Int. J. Thermophys., 2011, 34, 2243), as well as those obtained using the parachor method, were in good agreement with the measurement data.

## ■ INTRODUCTION

Climate change has become a critical issue worldwide that needs to be mitigated. The Kigali amendment<sup>1</sup> to the Montreal protocol declared a phase-down schedule for the production and consumption of hydro-fluoro-carbons (HFCs) and hydro-chloro-fluoro-carbons (HCFCs) used in heat pumps and organic Rankine cycles because of their high global warming potentials (GWPs). This has further motivated research on low-global-warming fluids. Unsaturated fluorinated compounds called hydro-fluoro-olefins (HFOs) and hydro-chloro-fluoro-olefins (HCFOs) have been identified as promising alternatives to HFCs and HCFCs owing to their extremely short atmospheric lifetime (typically less than 10 days) due to their reactivity with hydroxyl radicals in atmosphere. R1224yd(Z) has been nominated as the replacement for HFC-245fa<sup>2</sup>. This substance has only a slight ozone-depleting potential (ODP); nevertheless, it is considered suitable for use in industrial high-temperature heat pumps and organic Rankine cycles. In this manuscript, surface tension data are precisely measured using a differential capillary-rise-height method. Based on the data, the empirical correlations expressing the temperature dependence are obtained and the parachor is determined.

## ■ MEASUREMENT METHOD

### Measurement Setup

The differential capillary-rise-height method was used to determine the surface tension, which was developed by Sugden<sup>3</sup> and Richards and Speyers<sup>4</sup>. Figure 1 shows the measurement setup, originally developed by Okada et al.<sup>5</sup>. The surface tension was measured from the capillary elevation in three small-diameter tubes immersed in liquid. The capillary radii and their uniformity were precisely measured with mercury slugs by Okada et al.<sup>6</sup> for  $r_A$  and  $r_B$  and later measured by authors for  $r_C$ . The inner radii were  $r_A = 0.7526 \pm 0.0009$  mm,  $r_B = 0.4222 \pm 0.0009$  mm, and  $r_C = 0.248 \pm 0.002$  mm. These three glass capillaries were set up vertically using a polytetrafluoroethylene supporting brace in a pressure vessel (A) composed of a Pyrex glass tube with inner and outer diameters of 17 and 25 mm, respectively. These capillaries and pressure vessel were carefully cleansed with an alkaline aqueous solution and ultrasound bath in the preparatory procedure. The refrigerant liquid was filled to approximately half the volume of the pressure vessel at room temperature. Thereafter, the pressure vessel was placed in a well-insulated thermostatic bath (B) that could maintain the temperature with a fluctuation of within  $\pm 10$  mK by using a proportional–integral–derivative (PID) (K) controlled heater (F) and chiller (G). The temperature was measured with a 100- $\Omega$  platinum resistance thermometer (M) and data acquisition unit ASL model F500, which were calibrated against ITS-90. The uncertainty in the temperature measurement was estimated to be within  $\pm 5$  mK. At steady state, the capillary rise difference between the two capillary tubes was measured using a digital traveling microscope (L) with a 0.01-mm tolerance.

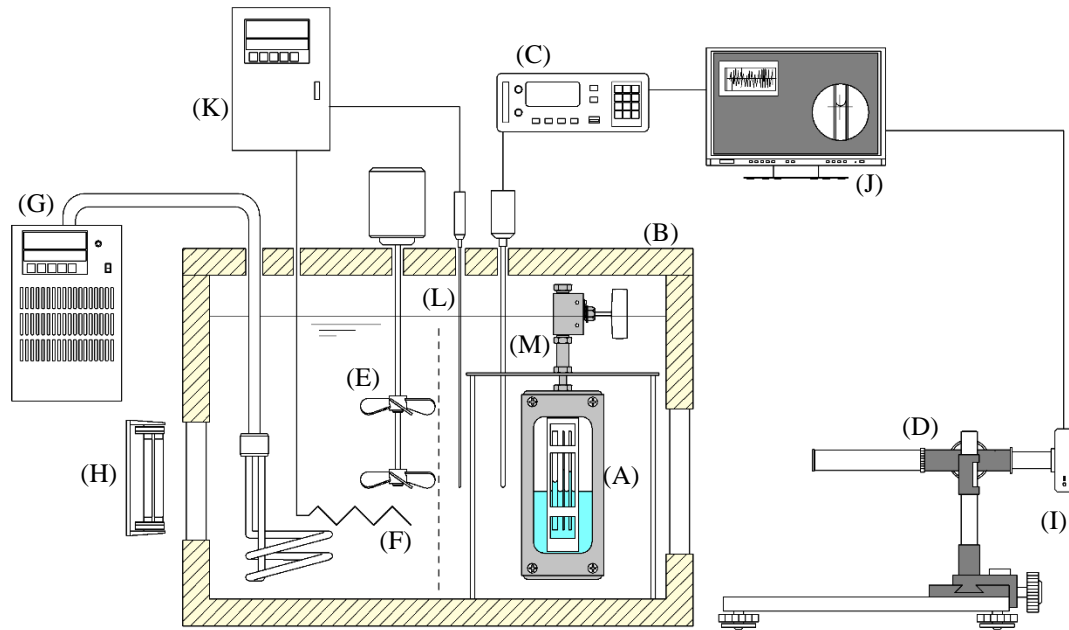


**Figure 1.** Measurement setup: (A) pressure vessel, (B) thermostatic bath, (C) thermometer bridge, (D) traveling microscope, (E) stirrer, (F) electric heater, (G) chiller, (H) LED illumination, (I) CCD camera, (J) computer, (K) PID temperature-control system, (L) sheathed thermocouple, and (M) platinum resistance thermometer (100  $\Omega$ ).

### Principle and Data-Reduction Method

Figure 2 illustrates the principle of the differential capillary-rise-height method. The height difference between the menisci bottoms of the adjacent capillary tubes were measured using the traveling microscope (D) and charge-coupled device (CCD) camera (I), as shown in Fig. 1. Thus, with three capillary tubes, three height differences were obtained simultaneously. The differential heights were read eight times by multiple people to avoid variations in individual readings. The two standard deviations among the eight readings were approximately  $\pm 0.04$  mm. This deviation

was considered in the uncertainty of the measurement of surface tension. To obtain the actual differential capillary rise height, the measured differential height,  $\Delta h_m$ , at the bottom of the meniscus in each capillary tube was corrected using the methodology of Rayleigh<sup>7</sup>, which is available for cases in which the observed meniscus curvature is nearly hemispherical.

$$\Delta h_c = \Delta h_m + \frac{r_1 - r_2}{3} - 0.1288 \left( \frac{r_1^2}{h_{m1}} - \frac{r_2^2}{h_{m2}} \right) + 0.1312 \left( \frac{r_1^3}{h_{m1}^2} - \frac{r_2^3}{h_{m2}^2} \right) + \dots \approx \Delta h_m + \frac{(r_1 - r_2)}{3} \quad (1)$$

where  $\Delta h_m$  is the measured height difference between the menisci bottoms.  $r_1$  and  $r_2$  are the capillary radii. The capillary constant,  $a^2$ , was determined only from the capillary radii,  $r_1$  and  $r_2$ , and corrected differential capillary rise height,  $\Delta h_c$ .

$$a^2 = \frac{g \Delta h_c}{g_n (1/r_1 - 1/r_2)} \quad (2)$$

where  $g$  and  $g_n$  are the local gravitational acceleration ( $9.79585 \text{ m} \cdot \text{s}^{-2}$ ) at Nagasaki City, Japan and normal gravitational acceleration ( $9.80665 \text{ m} \cdot \text{s}^{-2}$ ), respectively. Then, the surface tension  $\sigma$  is obtained from the capillary constant,  $a^2$ , as

$$\sigma = \frac{a^2 g_n (\rho' - \rho'')}{2} \quad (3)$$

where  $\rho'$  and  $\rho''$  are the orthobaric liquid and vapor densities, respectively.

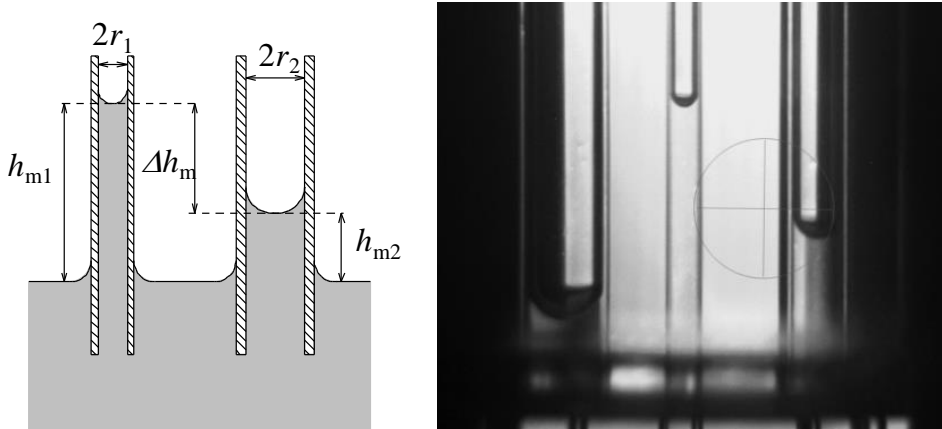


**Figure 2.** Principle of the differential capillary-rise-height method.  $\Delta h_m$  is the measured height difference between the menisci bottoms. The picture on the right-hand side is a typical CCD image displayed on a monitor to determine the position of the bottom of the hemispherical meniscus.

### Measurement Uncertainty

Table 1 summarizes the equipment and measurement uncertainties for each parameter. The calculation uncertainty for density was estimated to be 0.5%, according to the fluid information statement declared in REFPROP10<sup>8</sup> for R1224yd(Z). From the listed uncertainty sources in Table 1, the propagated measurement uncertainty with a 95% confidence level ( $k=2$ ) in surface tension is estimated to be within  $0.19 \text{ mN}\cdot\text{m}^{-1}$  in the range of measurement condition. The calculation procedure is specified in Appendix. The breakdown of uncertainty in surface tension at a typical condition, where a total uncertainty is  $0.18 \text{ mN}\cdot\text{m}^{-1}$ , is exemplified in Table 1. Obviously, the most dominant uncertainty source is the reading uncertainty in differential capillary rise height caused by the optical resolution limitation of traveling microscope. In the section of measurement results, the uncertainty value corresponding to each measurement data is specified in Table 5.

**Table 1.** Measurement uncertainties with a 95% confidence level in each factor that affects surface tension determination.

Parameter	Equipment/program	Uncertainty ( $k = 2$ )	
		Temperature (ITS-90)	Pt resistance and bridge, ASL F500
Differential capillary rise height, $\Delta h_m$	Digital traveling microscope, NRM-D-2XZ	0.05 mm (tolerance: 0.01mm)	$0.178 \text{ mNm}^{-1*}$ (98.8%)
Inner radii of the capillaries $r_A$ and $r_B$ $r_C$	Mercury slug method <sup>6</sup>	0.0009 mm 0.002 mm	$1 \times 10^{-3} \text{ mNm}^{-1*}$ (0.61%)
Orthobaric densities, $\rho'$ and $\rho''$	REFPROP 10.0 (Lemmon et al. <sup>8</sup> ) associated with the following equation of state: [R245fa] Akasaka et al. <sup>9</sup> [R1224yd(Z)] Akasaka <sup>10</sup>	0.5% of calculated values	$9 \times 10^{-4} \text{ mNm}^{-1*}$ (0.53%)

\*The uncertainties in unit of  $\text{mNm}^{-1}$  indicate the breakdown of the uncertainty in surface tension at the expanded uncertainty with a 95% level of confidence is  $0.18 \text{ mNm}^{-1}$ . The parenthesized percentages are the proportions in total uncertainty.

### Sample Refrigerant

Figure 3 shows the molecular structure and orthobaric density of R1224yd(Z). To determine the surface tension from the capillary constant, the equation of state (EOS) of Akasaka<sup>10</sup> was used to calculate the orthobaric densities  $\rho''$  and  $\rho'$  in Eq. (3). As shown in Fig. 3, the measured densities were in good agreement with the calculated densities. However, it should be noted that there are no available data at lower temperatures and the density is extrapolated below 280 K.

Table 2 lists the fundamental properties and sample purity of R1224yd(Z). The sample was provided by AGC Inc. According to the material sheet, the purity was more than 99.5%.

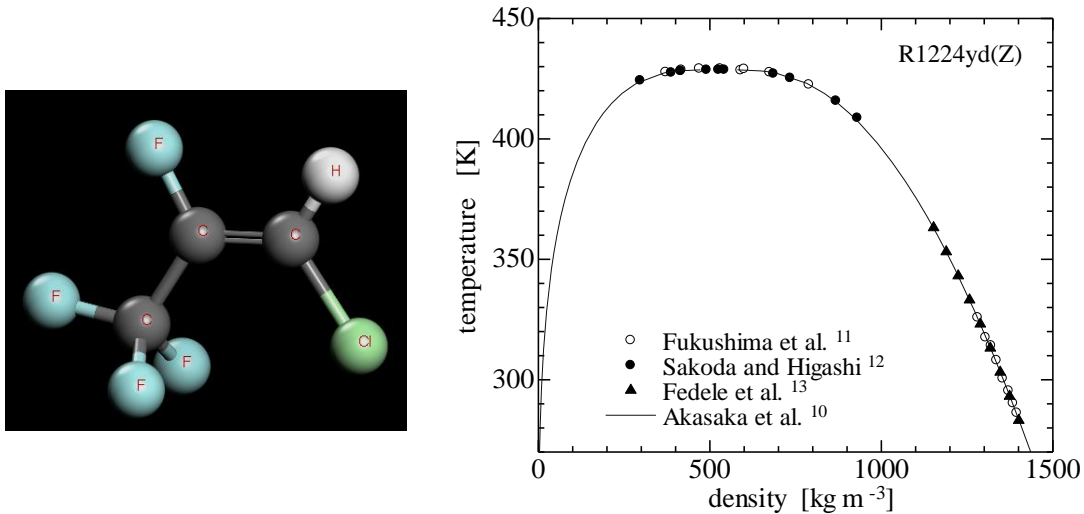


**Figure 3.** Molecular structure and available orthobaric density data for R1224yd(Z). The symbols represent the data obtained by Fukushima et al.<sup>11</sup>(○), Sakoda and Higashi<sup>12</sup> (●), and Fedele et al.<sup>13</sup>(▲), respectively. The line represents the values calculated using REFPROP 10 (Lemmon et al.<sup>8</sup>) associated with the EOS of Akasaka et al.<sup>10</sup>

**Table 2.** Specifications of the sample refrigerant R1224yd(Z).

Designation	HCFO-1224yd(Z)
CAS number	111512-60-8
Name	cis-1-chloro-2,3,3,3-tetrafluoropropene
NBP	287.2 K <sup>14</sup>
Critical temp.	428.69 ± 0.02 K <sup>12</sup>
ODP*	0.00012 <sup>14</sup>
GWP <sub>100</sub> **	<1 <sup>14</sup>
ASHRAE safety class <sup>15</sup>	A1 <sup>15</sup>
Purity	>99.5 mol%
Impurities	acids < 0.0001 mol% H <sub>2</sub> O < 0.002 mol% others < 0.5 mol%
*Ozone depletion potential	** Global warming potential of 100 year time horizon.



## ■ MEASUREMENT RESULTS

### Validation of measurement method

Figure 4 shows the surface tension measurement results of R245fa as a function of temperature, to ensure that the measurement method is valid. The R245fa sample data are specified in Table 3. The fluid R245fa was selected because it has thermophysical properties that are similar to those of the sample refrigerant. The symbols in the graph on the left-hand side of Fig. 4 represent the present and previously reported data from the literature<sup>16-20</sup> for comparison. The present data with respect to the capillary constant and surface tension are listed in Table 4. The line in Fig. 4 represents the surface tension calculated using the correlation of Mulero et al.<sup>21</sup> implemented in REFPROP10<sup>8</sup>. The graph on the right-hand side of Fig. 4 shows the deviation of the measurement data from the calculated surface tension. In the confirmed temperature range, the deviation is approximately within  $0.15 \text{ mN}\cdot\text{m}^{-1}$ , which is less than the uncertainty mentioned above. Overall, the repeatability and reproducibility in the R245fa surface tension data validate the measurement method.

**Table 3.** Specifications of the sample refrigerant R245fa

Designation	HFC-245fa
CAS number	460-73-1
Name	1,1,1,3,3-pentafluoropropane
NBP	288.198 K <sup>22</sup>
Critical temp.	427.01 K <sup>22</sup>
ODP*	0
GWP <sub>100</sub> **	858 <sup>23</sup>
ASHRAE safety class <sup>14</sup>	B1 <sup>24</sup>
Purity	>99.5 mol%
Impurities	N/A
Manufacturer	AGC Inc.
*Ozone depletion potential	** Global warming potential of 100 year time horizon.

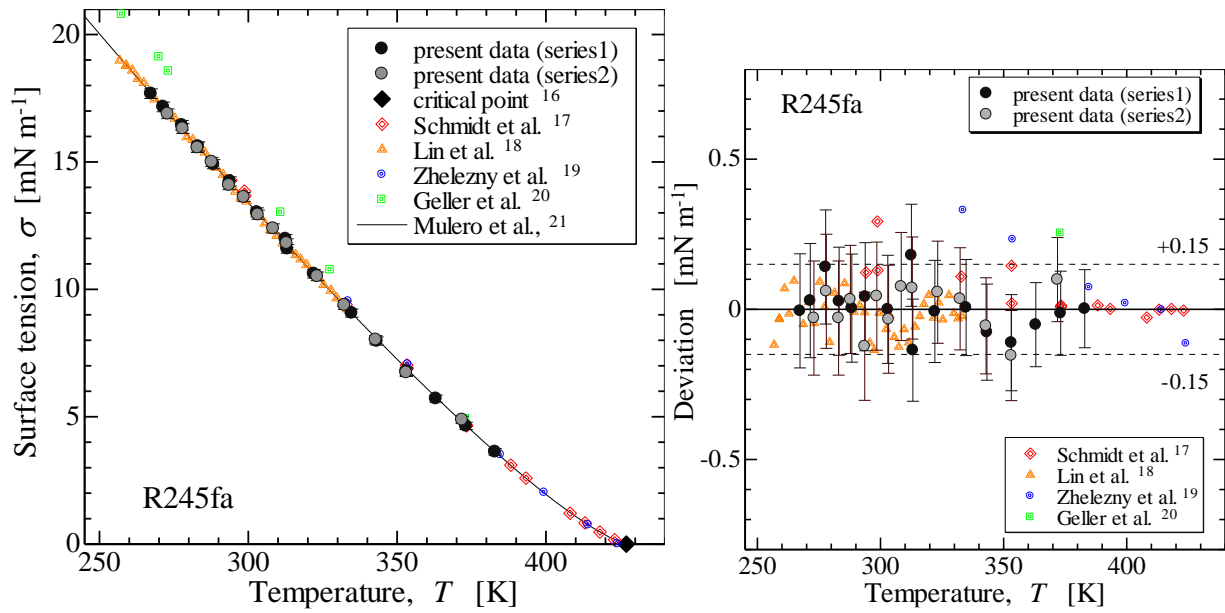


**Figure 4.** (left) Measured R245fa surface tension obtained in the present work and previous work reported in the literature<sup>16–20</sup>. (right) Deviation from the results obtained using the correlation of Mulero et al.<sup>21</sup>.

**Table 4.** Measured capillary constant and surface tension for R245fa.

Series	Temperature (ITS-90)	Vapor <sup>*a</sup> density	Liquid <sup>*a</sup> density	Capillary constant	Surface tension	Uncertainty <sup>*b</sup> ( $k = 2$ )
	[K]	[kg·m <sup>-3</sup> ]	[kg·m <sup>-3</sup> ]	[mm <sup>2</sup> ]	[mN·m <sup>-1</sup> ]	[mN·m <sup>-1</sup> ]
1	267.32	2.50	1418.59	2.55	17.68	0.19
	271.47	3.00	1408.16	2.49	17.16	0.19
	277.73	3.92	1392.23	2.41	16.44	0.19
	283.18	4.89	1378.17	2.32	15.61	0.18
	288.35	5.98	1364.65	2.24	14.91	0.18
	293.81	7.32	1350.17	2.16	14.24	0.18
	302.97	10.11	1325.30	2.02	13.02	0.18
	312.56	13.86	1298.40	1.90	11.98	0.17
	313.15	14.12	1296.70	1.84	11.59	0.17
	322.07	18.60	1270.71	1.73	10.61	0.17
	334.76	26.87	1231.85	1.53	9.07	0.16
	343.24	33.90	1204.43	1.39	7.97	0.16
	353.15	44.01	1170.48	1.23	6.78	0.16
	363.08	56.66	1134.01	1.08	5.71	0.14
	373.17	72.81	1093.60	0.93	4.64	0.14
382.94	92.62	1050.27	0.77	3.62	0.13	
2	272.96	3.21	1404.38	2.48	16.89	0.19
	278.00	3.96	1391.54	2.41	16.31	0.19
	282.98	4.84	1378.70	2.32	15.56	0.19
	287.77	5.82	1366.19	2.25	15.00	0.18
	293.59	7.23	1350.76	2.13	14.09	0.18
	298.52	8.61	1337.47	2.08	13.62	0.18
	303.29	10.15	1324.41	1.99	12.93	0.18
	308.40	12.03	1310.17	1.93	12.39	0.18
	312.93	13.92	1297.33	1.85	11.81	0.17
	323.23	19.09	1267.25	1.68	10.51	0.17
	332.33	24.86	1239.48	1.52	9.38	0.17
	342.86	33.26	1205.67	1.33	8.02	0.16
	353.12	43.61	1170.60	1.13	6.73	0.15
	371.88	70.12	1099.01	0.85	4.88	0.14

\*a Calculated using REFPROP10<sup>8</sup> with EOS of Akasaka et al.<sup>22</sup>

\*b Expanded uncertainty for a 95% level of confidence ( $k = 2$ )

### R1224yd(Z) surface tension

Figure 5 plots the three series of surface tension measured for R1224yd(Z) as a function of temperature. The data of series 1, 2, and 3 strongly overlap within the measurement uncertainty, which is estimated to be less than  $0.19 \text{ mN}\cdot\text{m}^{-1}$ . Table 5 lists the capillary constant and surface tension, and also the density data of 26 points at temperatures ranging from 266 K to 373 K. Based on these data, the following van der Waals-type correlation is proposed.

$$\sigma_{\text{R1224yd(Z)}} = 57.02 \times 10^{-3} \left( 1 - \frac{T}{T_{\text{crit}}} \right)^{1.265} \quad [\text{N m}^{-1}], \quad T_{\text{crit}} = 428.69 \text{ [K]} \quad (4)$$

where  $T$  is the temperature in K.  $T_{\text{crit}}$  is the critical temperature of 428.69 K reported by Higashi and Akasaka<sup>12</sup>. The coefficient 57.02 and exponent 1.265 are determined from the measurement results, using the least-square-mean method. The line in Fig. 5 indicates the above correlation, which represents the measurement results within  $0.15 \text{ mN}\cdot\text{m}^{-1}$ .

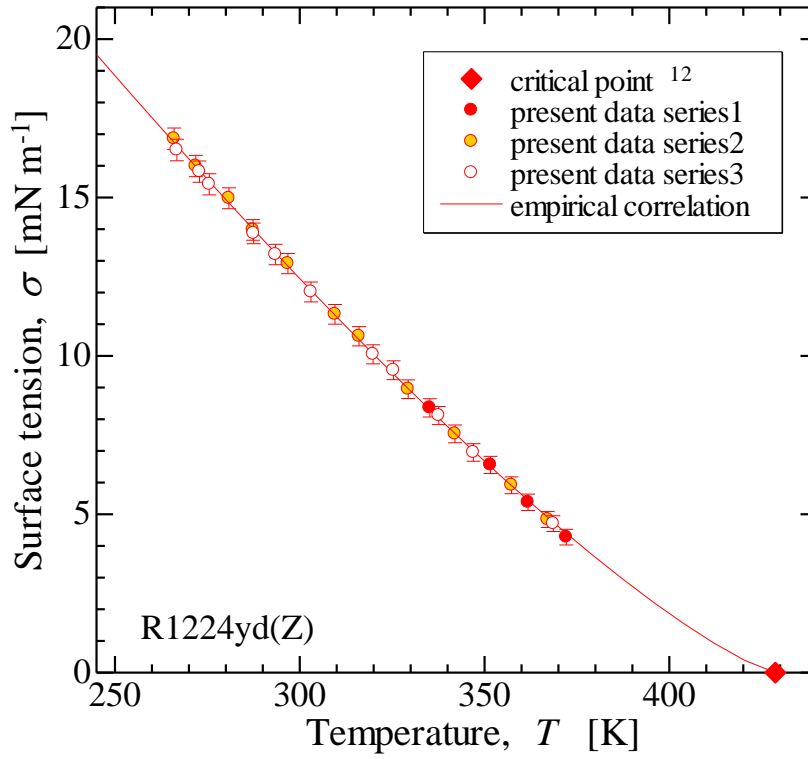


**Figure 5.** Temperature dependence of the measured surface tension. The diamond symbol indicates the critical temperature of 428.69 K reported by Higashi and Akasaka<sup>12</sup>. The line represents the empirical correlation of the surface tension with the critical temperature.

**Table 5.** Measured capillary constant and surface tension for R1224yd(Z).

Series	Temperature (ITS-90)	Vapor* <sup>a</sup> density	Liquid* <sup>a</sup> density	Capillary constant	Surface tension	Uncertainty* <sup>b</sup> ( $k = 2$ )
	[K]	[kg·m <sup>-3</sup> ]	[kg·m <sup>-3</sup> ]	[mm <sup>2</sup> ]	[mN·m <sup>-1</sup> ]	[mN·m <sup>-1</sup> ]
1	335.17	28.63	1250.64	1.40	8.36	0.17
	351.60	43.84	1194.71	1.16	6.56	0.16
	361.77	56.40	1156.96	1.00	5.38	0.15
	372.13	72.47	1115.34	0.84	4.28	0.14
2	266.00	2.79	1445.76	2.38	16.85	0.19
	271.89	3.57	1430.83	2.29	15.99	0.19
	280.83	5.10	1407.69	2.18	14.97	0.19
	287.34	6.50	1390.47	2.06	13.98	0.19
	296.79	9.05	1364.84	1.94	12.91	0.18
	309.52	13.67	1328.97	1.76	11.31	0.18
	316.03	16.67	1309.95	1.68	10.62	0.18
	329.35	24.42	1269.28	1.47	8.95	0.17
	342.00	34.30	1228.05	1.29	7.54	0.16
	357.30	50.53	1173.89	1.08	5.92	0.15
	367.09	64.18	1136.04	0.92	4.83	0.15
	3	287.51	6.54	1390.01	2.05	13.87
303.04		11.13	1347.45	1.84	12.02	0.18
319.83		18.64	1298.59	1.60	10.05	0.17
272.87		3.72	1428.30	2.27	15.82	0.19
275.52		4.14	1421.49	2.22	15.42	0.19
266.74		2.88	1443.88	2.34	16.49	0.19
293.45		8.07	1373.99	1.97	13.20	0.19
325.37		21.86	1281.67	1.55	9.55	0.17
337.62		30.56	1242.65	1.37	8.12	0.17
346.99		39.01	1210.98	1.21	6.95	0.16
368.60		66.57	1129.93	0.90	4.70	0.15

\*a Calculated using REFPROP10<sup>8</sup> with EOS of Akasaka et al.<sup>10</sup>\*b Expanded uncertainty for a 95% level of confidence ( $k = 2$ )

### **R1224yd(Z) parachor**

The parachor method proposed by Macleod<sup>25</sup> has been used to estimate the surface tension from liquid and vapor densities.

$$\sigma = [[P](\rho' - \rho'')]^4 \quad (5)$$

where  $\sigma$  is the surface tension in  $\text{dyn}\cdot\text{cm}^{-1}$  or  $\text{mN}\cdot\text{m}^{-1}$ ,  $\rho'$  and  $\rho''$  are the liquid and vapor densities in  $\text{mol}\cdot\text{cm}^{-3}$ , respectively, and  $[P]$  is the inherent parameter, called parachor, that depends on the molecular structure. Figure 6 plots the parachor obtained from the surface tension data for R245fa and R1224yd(Z). The symbols are obtained from the present work and the previous works performed by previous researchers<sup>17-20, 26</sup> on R245fa. In the earlier works, the parachor was considered a temperature-independent parameter. However, most R245fa parachor data slightly decreases below 370 K. A sudden increase can be observed close to the critical temperature in the data of Schmidt et al.,<sup>17</sup> Zhelezny et al.,<sup>19</sup> and the present work. The temperature dependence of parachor was suggested by Zhelezny et al.,<sup>27</sup>. According to their work, the parachor at the critical temperature of 427.01 K was 199.0, which is somewhat higher than the value shown below 370 K. The accuracy at lower temperatures was even more important in the prediction of the surface tension; at lower temperatures, the surface tension value becomes higher. Therefore, by eliminating the data near the critical point, the parachor is determined as 194 for R245fa. In the present parachor data of R1224yd(Z), a slight decrease can be observed; however, a sudden increase was not observed. Thus, by simple averaging, the parachor was determined as 207 for R1224yd(Z).

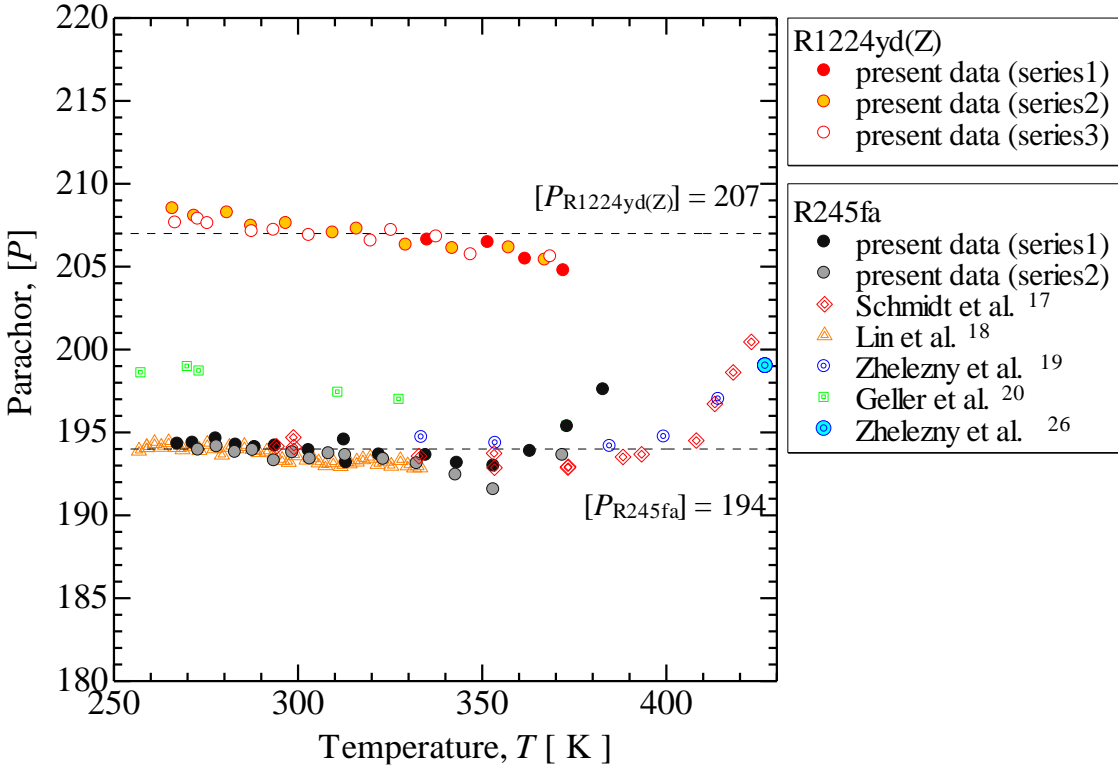


**Figure 6.** Obtained parachor  $[P]$  values from Eq. (5) for R245fa and 1224yd(Z). The parachor values were obtained from the surface tension data of present and previous works<sup>17–20, 26</sup>. It is determined as 194 and 207 for R245fa and R1224yd(Z), respectively.

### 1224yd(Z) surface tension prediction

Figure 7 compares the measured R1224yd(Z) surface tension with the predicted surface tension. The measurement data were in good agreement with the predicted surface tension values. The parachor was determined from the measurement data; thus, the results of the parachor method were in good agreement with the measurement data within the uncertainty. To show the comparison in detail, the deviation from the proposed empirical correlation Eq. (4) is shown in Fig. 8. The measurement data were in good agreement with the empirical correlation within the estimated measurement uncertainty of 95% confidence. The predictions of Miqueu et al.<sup>28</sup>, Miller and



Thodos<sup>29</sup>, and Di Nicola et al.<sup>30</sup> were in good agreement with the measurement data within the uncertainty.

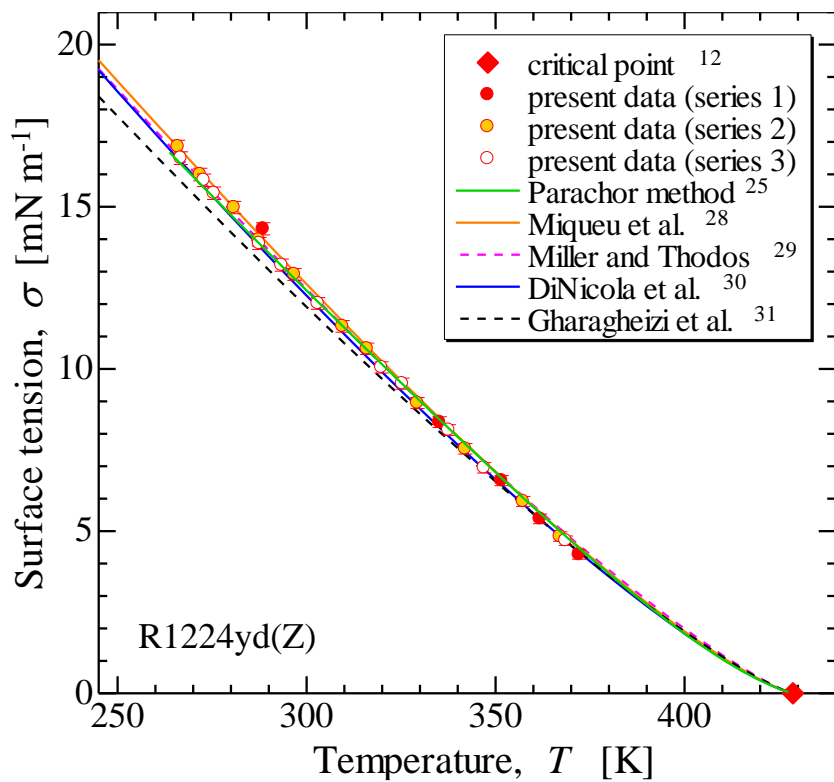


**Figure 7.** Comparison between measured and predicted R1224yd(Z) surface tension. Lines represent the values predicted by Miller and Thodos<sup>29</sup>, Miqueu et al.<sup>28</sup>, Di Nicola et al.<sup>30</sup>, and Gharagheizi et al.<sup>31</sup>, as well as those obtained with the parachor method<sup>25</sup>.

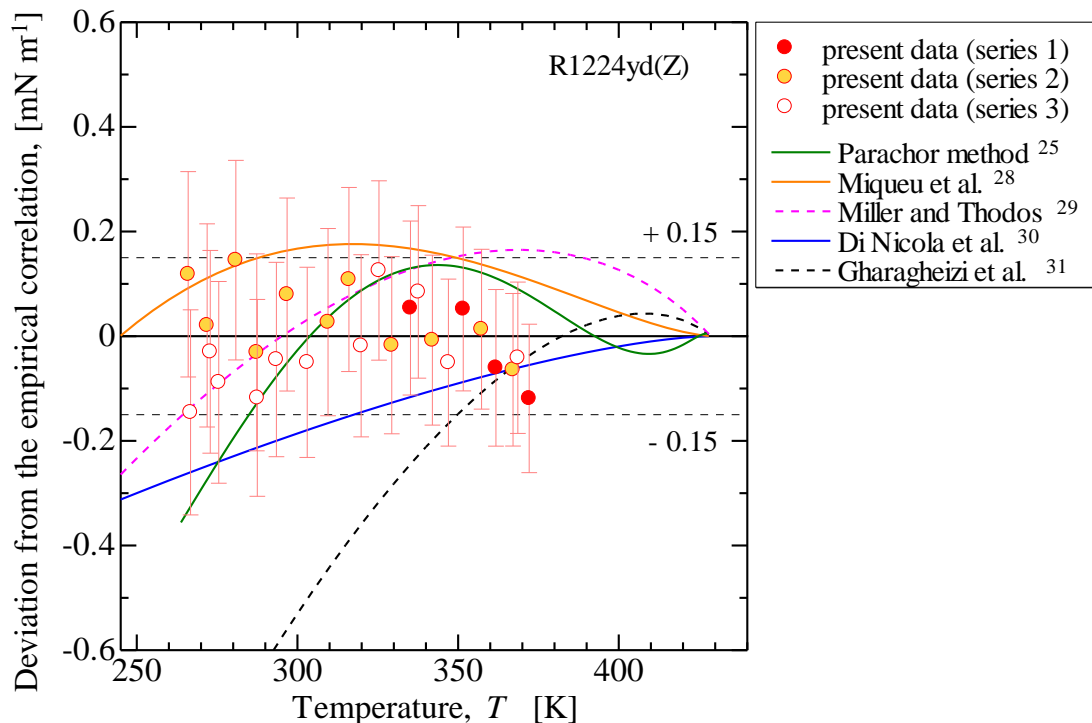


**Figure 8.** Deviation from the empirical correlation Eq. (4). Symbols represent the present measurement data, and the appended vertical bars represent the measurement uncertainty. Lines represent the predictions developed by Miller and Thodos<sup>29</sup>, Miqueu et al.<sup>28</sup>, Di Nicola et al.<sup>30</sup>, and Gharagheizi et al.<sup>31</sup>, as well as the values obtained using the parachor method<sup>25</sup>.

## ■ CONCLUSIONS

The surface tension of *cis*-1-chloro-2,3,3,3-tetrafluoropropene (R1224yd(Z), (Z)-CF<sub>3</sub>CF=CHCl) has been measured over the temperature range 266–340 K with uncertainty within  $\pm 0.19$  mN·m<sup>-1</sup>. This was slightly lower than the measured surface tension of R245fa. Based on the measurement data, an empirical correlation was obtained as  $\sigma = 57.02 (1-T/428.69)^{1.265}$  [mN·m<sup>-1</sup>] and the

parachor was determined as 207 for R1224yd(Z). The predictions developed by Miller and Thodos, Miqueu et al., and Di Nicola et al. were in good agreement with the measurement data.

## ■ AUTHOR INFORMATION

### **Corresponding Author**

\*E-mail: ckondou@nagasaki-u.ac.jp

### **ORCID**

Chieko Kondou: 0000-0002-0504-3048

### **Funding Sources**

This study was financially supported by the JSPS KAKENHI Grant Number 17K14603 and Asahi Glass Co., Ltd., Japan.

## ■ ACKNOWLEDGMENT

The sample refrigerants were kindly donated by Asahi Glass Co., Ltd., Japan. This study was financially supported by the JSPS KAKENHI Grant Number 17K14603. The authors are grateful for their support.

■ APPENDIX: UNCERTAINTY CALCULATION PROCEDURE

The calculation procedure of measurement uncertainty in surface tension is described here. Substituting  $a^2$  in Eq. (3) by Eq. (2), the surface tension measured by capillaries of 1 and 2,  $\sigma_{12}$ , is rewritten as,

$$\sigma_{12} = \frac{g \cdot \Delta h_c}{2(1/r_1 - 1/r_2)} (\rho' - \rho'') \quad (\text{A1})$$

Thus, the 95% coverage of uncertainty propagated by the variables  $\rho'$ ,  $\rho''$ ,  $r_1$ ,  $r_2$ , and  $\Delta h_c$  is estimated by means of the square-root rule<sup>32,33</sup>.

$$U_{\sigma_{12}} = \sqrt{\left(\frac{\partial \sigma_{12}}{\partial \rho'} U_{\rho'}\right)^2 + \left(\frac{\partial \sigma_{12}}{\partial \rho''} U_{\rho''}\right)^2 + \left(\frac{\partial \sigma_{12}}{\partial r_1} U_{r_1}\right)^2 + \left(\frac{\partial \sigma_{12}}{\partial r_2} U_{r_2}\right)^2 + \left(\frac{\partial \sigma_{12}}{\partial \Delta h_c} U_{\Delta h_c}\right)^2} \quad (\text{A2})$$

where,

$$\frac{\partial \sigma_{12}}{\partial \rho'} = \frac{g \cdot \Delta h_c}{2(1/r_1 - 1/r_2)} \quad (\text{A3})$$

$$\frac{\partial \sigma_{12}}{\partial \rho''} = -\frac{g \cdot \Delta h_c}{2(1/r_1 - 1/r_2)} \quad (\text{A4})$$

$$\frac{\partial \sigma_{12}}{\partial r_1} = -\frac{g \cdot \Delta h_c}{2r_1^2 (1/r_1 - 1/r_2)^2} (\rho' - \rho'') \quad (\text{A5})$$

$$\frac{\partial \sigma_{12}}{\partial r_2} = \frac{g \cdot \Delta h_c}{2r_2^2 (1/r_1 - 1/r_2)^2} (\rho' - \rho'') \quad (\text{A6})$$

$$\frac{\partial \sigma_{12}}{\partial \Delta h_c} = \frac{g}{2(1/r_1 - 1/r_2)} (\rho' - \rho'') \quad (\text{A7})$$

The uncertainty in each variable is as listed in Table 1. The uncertainty in corrected differential capillary rise height,  $U_{\Delta h_c}$ , in Eq. (A2) is assumed to be the same as the uncertainty in measured differential capillary rise height,  $U_{\Delta h_m}$ , listed in Table 1.

The uncertainties in surface tensions measured by capillary tubes of A and B,  $\sigma_{AB}$ , of B and C,  $\sigma_{BC}$ , and of A and C,  $\sigma_{AC}$ , are obtained using the above calculation procedure. The uncertainty in the representative surface tension value,  $\sigma = (\sigma_{AB} + \sigma_{BC} + \sigma_{AC})/3$ , is calculated from those three uncertainties as,

$$U_{\sigma} = \sqrt{\left(\frac{U_{\sigma_{AB}}}{3}\right)^2 + \left(\frac{U_{\sigma_{BC}}}{3}\right)^2 + \left(\frac{U_{\sigma_{AC}}}{3}\right)^2} \quad (\text{A8})$$

## ■ REFERENCES

- (1) Clark, E.; Wagner, S. The Kigali Amendment to the Montreal Protocol: HFC Phase-down. *Ozone Action Fact Sheet*, Kigali, Rwanda, **2016**.
- (2) Eyerer, S.; Dawo, F.; Kaindl, J.; Wieland, C.; Spliethoff, H. Experimental Investigation of Modern ORC Working Fluids R1224yd(Z) and R1233zd(E) as Replacements for R245fa. *Appl. Energy*, **2019**, 240, 946–963. doi:org/10.1016/j.apenergy.2019.02.086.
- (3) Sugden, S. The determination of surface tension from the rise in capillary tubes. *J. Chem. Soc. Trans.*, **1921**, 119, 1483-1492. doi:10.1039/CT9211901483
- (4) Richards, T. W.; Speyers, C. L.; Carver, E. K. The Determination of Surface Tension with Very Small Volumes of Liquid, and the Surface Tensions of Octanes and Xylenes at Several Temperatures. *J. Am. Chem. Soc.* **1924**, 46, 1196–1207. https://doi.org/10.1021/ja01670a012.
- (5) Okada, M.; Arima, T.; Hattori, M.; Watanabe, K. Measurements of the Surface Tension of Three Refrigerants, R 22, R 115, and R 502. *J. Chem. Eng. Data*, **1988**, 33, 399–401. https://doi.org/10.1021/je00054a003.
- (6) Oakada, M. Study on saturated liquid density and surface tension of fluorocarbon refrigerants. *Keio Univerisity, PhD thesis*, 1981.
- (7) Rayleigh, L. On the Theory of the Capillary Tube. *Proc. R. Soc. A Math. Phys. Eng. Sci.* **1916**, 92, 184–195. https://doi.org/10.1098/rspa.1916.0004.

- (8) Lemmon, E.W.; Bell, I.H.; Huber, M.L.; McLinden, M.O. *NIST Standard Reference Database 23, Reference Fluid Thermodynamic and Transport Properties-REFPROP*, Version 10.0, Standard Reference Data Program; National Institute of Standards and Technology: Gaithersburg, MD, USA, 2018.
- (9) Akasaka, R.; Zhou, Y.; Lemmon, E.W. A Fundamental Equation of State for 1,1,1,3,3-Pentafluoropropane (R-245fa). *J. Phys. Chem. Ref. Data*, **2015**, 44(1), 013104. doi: 10.1063/1.4913493.
- (10) Akasaka, R.; Fukushima, M.; Lemmon, E.W. A Helmholtz Energy Equation of State for cis-1-chloro-2,3,3,3-Tetrafluoropropene (R-1224yd(Z)). *European Conference on Thermophysical Properties*, Graz, Austria, 2017.
- (11) Fukushima, M.; Hayamizu, H.; Hashimoto, M. Thermodynamic Properties of Low-GWP Refrigerant for Centrifugal Chiller. *16th Int. Refrig. Air Cond. Conf.* **2016**, 2151, 1–10.
- (12) Sakoda, N.; Higashi, Y. Measurements of PvT Properties, Vapor Pressures, Saturated Densities, and Critical Parameters for Cis -1-Chloro-2,3,3,3-Tetrafluoropropene (R1224yd(Z)). *J. Chem. Eng. Data*, **2019**, (in press). doi: 10.1021/acs.jced.9b00374.
- (13) Fedele, L.; Boobo, S.; Scattolini, M.; Zilio, C.; Akasaka, R. Compressed Liquid Density Measurements and Correlation for Cis-1- chloro-2,3,3,3 tetrafluoropropene (R1224yd(Z)), *25th IIR International Congress of Refrigeration*, Montreal, Canada, **2019**, Manuscript ID 234, 1-8. doi:10.18462/iir.icr.2019.0234
- (14) AGC technical report, <http://www.agc-chemicals.com/file.jsp?id=30214>.
- (15) Designation and Safety Classification of Refrigerants, the latest edition of Standard 34. *ANSI/ASHRAE 34-2019*.
- (16) Higashi, Y.; Hayasaka, S.; Shirai, C.; Akasaka, R. Measurements of PpT Properties, Vapor Pressures, Saturated Densities, and Critical Parameters for R 1234ze(Z) and R 245fa. *Int. J. Refrig.* **2015**, 52, 100–108. <https://doi.org/10.1016/j.ijrefrig.2014.12.007>.

- (17) Schmidt, J.W.; Carrillo-Nava, E.; Moldover, M.R. Partially halogenated hydrocarbons CHFCl-CF<sub>3</sub>, CF<sub>3</sub>-CH<sub>3</sub>, CF<sub>3</sub>-CHF- CHF<sub>2</sub>, CF<sub>3</sub>-CH<sub>2</sub>-CF<sub>3</sub>, CHF<sub>2</sub>-CF<sub>2</sub>-CH<sub>2</sub>F, CF<sub>3</sub>-CH<sub>2</sub>-CHF<sub>2</sub>, CF<sub>3</sub>-O- CHF<sub>2</sub>: critical temperature, refractive indices, surface tension and estimates of liquid, vapor and critical densities. *Fluid Ph. Equilibria*, **1996**, 112, 187-206.
- (18) Lin, H.; Duan, Y.-Y.; Wang, Z.-W. Surface Tension Measurements of 1,1,1,3,3-Pentafluoropropane (HFC-245fa) and 1,1,1,3,3,3-Hexafluoropropane (HFC-236fa) from 254 to 333 K. *Fluid Ph. Equilibria*, **2003**, 214, 79–86. [https://doi.org/10.1016/S0378-3812\(03\)00316-9](https://doi.org/10.1016/S0378-3812(03)00316-9).
- (19) Zhelezny, V. P.; Semenyuk, Y. V.; Ancherbak, S. N.; Grebenkov, A. J.; Beliayeva, O. V. An Experimental Investigation and Modelling of the Solubility, Density and Surface Tension of 1,1,1,3,3-Pentafluoropropane (R-245fa)/Synthetic Polyolester Compressor Oil Solutions. *J. Fluor. Chem.* **2007**, 128, 1029–1038. <https://doi.org/10.1016/j.jfluchem.2007.05.011>.
- (20) Geller, Z.; Bivens, D.; Yokozeki, A. Transport properties and surface tension of hydrofluorocarbons HFC 236fa and HFC 245fa. In: *Proc. 20th Int. Congress of Refrigeration vol. II. IIR/ IIF*, **1999**, Paper no. 027, Sydney.
- (21) Mulero, A.; Cachadi, I.; Parra, M.I. Recommended Correlations for the Surface Tension of Common Fluids. *J. Phys. Chem. Ref. Data*, 41, 043105, 2012. doi: 10.1063/1.4768782.
- (22) Akasaka, R.. Thermodynamic property models for the difluoromethane (R-32)+trans-1,3,3,3-tetrafluoropropene (R-1234ze(E)) and difluoromethane+2,3,3,3-tetrafluoropropene (R-1234yf) mixtures. *Fluid Phase Equilib.* **2013** 358, 98–104. <https://doi.org/10.1016/j.fluid.2013.07.057>
- (23) Myhre, G.; Shindell, D.; Bréon, F.M.; Collins, W.; Fuglestedt, J.; Huang, J.; Koch, D.; Lamarque, J.F.; Lee, D.; Mendoza, B.; Nakajima, T.; Robock, A.; Stephens, G.; Takemura, T.; Zhan, H.; Anthropogenic and Natural Radiative Forcing, *Climate Change 2013: The Physical Science Basis. Contribution of Working Group I to the Fifth Assessment Report of the Intergovernmental Panel on Climate Change*, **2013**.

- (24) Designation and Safety Classification of Refrigerants, Addenda v and w to *ANSI/ASHRAE Standard 34-2004*.
- (25) Macleod, D. B. On a relation between surface tension and density. *Transactions of the Faraday Society*, **1923**, 19, 38-41.
- (26) Zhelezny, V.; Sechenyh, V.; Nikulina, A. A New Scaling Principles-Quantitative Structure Property Relationship Model (SP-QSPR) for Predicting the Physicochemical Properties of Substances at the Saturation Line. *J. Chem. Eng. Data*, **2014**, 59, 485-493. <https://doi.org/10.1021/je400933x>.
- (27) Zhelezny, V. P.; Semenyuk, Y. V.; Ancherbak, S. N.; Emel'yanenko, N. V. The Temperature Dependence of Parachor. *Russ. J. Phys. Chem. A*, **2009**, 83, 182-186. doi:10.1134/s0036024409020071.
- (28) Miqueu, C.; Broseta, D.; Satherley, J.; Mendiboure, B.; Lachaise, J.; Graciaa, A. An extended scaled equation for the temperature dependence of the surface tension of pure compounds inferred from an analysis of experimental data. *Fluid Ph. Equilibria*, **2000**, 172, 169-182.
- (29) Miller, D. G.; Thodos, G. Correspondence on the Reduced Frost-Kalkwarf Vapor Pressure Equation. *Ind. Eng. Chem. Fund.*, **1963**, 2.1, 78-80.
- (30) Di Nicola, G.; Di Nicola, C.; Moglie, M. A New Surface Tension Equation for Refrigerants. *Int. J. Thermophys.* **2011**, 34, 2243-2260.
- (31) Gharagheizi, F.; Eslamimanesh, A.; Sattari, M.; Mohammadi, A.H.; Richon, D. Development of corresponding states model for estimation of the surface tension of chemical compounds. *AIChE J*, **2013**, 59, 613-621.
- (32) Taylor, J.T. An Introduction to Error Analysis, second ed. *University science book*, **1982**, 45-79.
- (33) Moffat, R. J. Describing the Uncertainties in Experimental Results. *Exp. Therm. Fluid Sci.* **1988**, 1, 3-17.



For Table of Contents Only

